PAPER

Check for updates

Impact of different soil solutions on the stability and photocatalytic activity of commercial zinc oxide nanoparticles†

Karolina Solymos,[ab] Eszter Kanász,[a] Áron Ágoston, [iD][ac] Tamás Gyulavári, [iD][a] Benjámin Pálffy,[b] Ákos Szamosvölgyi,[a] Ákos Kukovecz, [iD][a] Zoltán Kónya [iD][a] and Zsolt Pap [iD] *[ade]

Zinc oxide (ZnO) nanoparticles are extensively utilized across various industries due to their versatile applications. However, the widespread use of these nanoparticles raises concerns regarding their potential release into soil environments, and also into the soil solution. Therefore, this study aims to delve into the interplay between different soil solution properties and the stability as well as photocatalytic activity of commercially available ZnO nanoparticles. It is observed that these interactions precipitate a reduction in the primary crystallite sizes of ZnO, primarily attributed to the release of Zn^{2+} ions under acidic conditions, and the formation of zinc complexes or hydroxides in alkaline environments. In acidic media, there is a concomitant decrease in the hydrodynamic diameter of ZnO, serving as further confirmation of Zn^{2+} release, which is corroborated by analytical measurements. Conversely, in alkaline media, the hydrodynamic diameter remains unaltered, suggesting the formation of an amorphous layer on the nanoparticle surface in such conditions. Further analyses into the surface chemistry of ZnO nanoparticles reveal the adsorption of various organic substances onto their surfaces. These organic compounds potentially function as electron traps or occupy active sites, however, after the interaction with soil solutions, the material was still able to degrade the model pollutant. So, the interaction with soil solutions reduced the activity, but the catalyst retained its efficiency. In essence, this study underscores the importance of comprehensively understanding the behavior of ZnO nanoparticles in soil environments. Such insights are pivotal for informed decision-making regarding the sustainable utilization of ZnO nanoparticles across various industrial domains.

Environmental significance

ZnO nanoparticles are widely employed in diverse industries for their versatile applications, but their extensive use raises concerns about potential release into soil environments and the soil solution. Therefore, understanding how these nanoparticles interact with soil solution properties, change in size, and retain their photocatalytic activity is crucial for assessing their potential environmental impacts. The findings shed light on how ZnO nanoparticles may behave in natural settings, influencing their potential mobility, reactivity with organic matter, and risks of contamination in soil and groundwater. This knowledge is essential for informed decision-making regarding the safe and sustainable use of ZnO nanoparticles across various industries, contributing to environmental protection and human health.

[a] Department of Applied and Environmental Chemistry, University of Szeged, Rerrich B. Sqr. 1, Szeged, HU-6720, Hungary. E-mail: pzsolt@chem.u-szeged.hu
[b] Department of Geoinformatics, Physical and Environmental Geography, University of Szeged, Egyetem Str. 2–6, Szeged, HU-6722, Hungary
[c] Department of Physical Chemistry and Materials Sciences, University of Szeged, Rerrich B. Sqr.1, Szeged, HU-6720, Hungary
[d] Nanostructured Materials and Bio-Nano-Interfaces Center, Institute for Interdisciplinary Research on Bio-Nano-Sciences, Babeş–Bolyai University, Treboniu Laurian Str. 42, Cluj-Napoca, RO-400271, Romania
[e] Institute of Research-Development-Innovation in Applied Natural Sciences, Babeş–Bolyai University, Treboniu Laurian Str. 42, Cluj-Napoca, RO-400271, Romania
† Electronic supplementary information (ESI) available. See DOI: https://doi.org/10.1039/d4en00354c

1. Introduction

Zinc oxide nanoparticles (ZnO NPs) are widely used semiconductors, mostly applied in the following areas: concrete and rubber fabrication,[1] the optoelectronic industry,[2] gas-sensing, cosmetics,[3] the textile industry,[4] medical applications,[5] agriculture,[6] and as a photocatalyst.[7] Concrete can be eroded slowly,[8] providing a constant source of ZnO NPs in a built environment. Rubber waste is a big issue as just a small fraction of it is recyclable.[9] Cosmetics are known to contain a high amount of ZnO as a coloring agent and disinfectant; even in the EU, where ZnO NPs are

1328 | *Environ. Sci.: Nano*, 2025, **12**, 1328–1339

This journal is © The Royal Society of Chemistry 2025

allowed to be used, they are introduced into the environment constantly *via* wastewater. Textiles with ZnO NPs are also used, while different electronic devices containing ZnO can end up as Waste from Electrical and Electronic Equipment (WEEE).[4] According to estimates to date, environmental concentrations of ZnO NPs have been increasing over the years. Already in 2009, 0.24–0.661 µg kg^{-1} and 0.22–1.42 µg L^{-1} ZnO NPs were measured in the soil and in water treatment plant effluent in Switzerland, respectively.[10] However, potential negative effects, which may result from the interaction of ZnO with the soil, are often ignored.

The presence of ZnO NPs in soil poses significant risks to organisms due to their potential toxicity.[11] Studies have shown that these NPs can accumulate in various organisms, leading to adverse effects on growth, reproduction, and overall ecosystem health.[12] Additionally, ZnO NPs have been found to induce oxidative stress and inflammation in exposed organisms, further exacerbating their harmful impact.[13]

Previous studies have investigated the behavior of various NPs in soil solutions. Specifically, a study highlights the distinctive traits of TiO$_2$ NPs in environments with high organic matter, demonstrating increased mobility within the media despite the abundant organic content.[14] Moreover, TiO$_2$ NPs retain their photocatalytic activity irrespective of the composition of the soil solution.[15,16] In another study, the influence of pH and dissolved organic matter (DOM) on the behavior of ZnO NPs is emphasized, revealing that negatively charged NPs exhibit higher total Zn concentrations at elevated pH levels.[17] Additionally, investigations into the interaction between CuO NPs and DOM indicate that hydrophobic DOM is more effective in stabilizing CuO NPs compared to hydrophilic DOM, especially in the presence of Ca^{2+}.[18]

ZnO NPs can enter the soil through multiple routes, including direct application,[19] atmospheric deposition,[20] and disposal in landfills.[21] They can also end up in wastewater through domestic use,[22] eventually entering sewage sludge,[23] which is commonly used as a soil fertilizer.[24] NPs that may persist at the soil surface, either within the pore water or attached to soil particles are influenced by the dynamic interplay between the solid and liquid phases of the soil. Retention and its rate are contingent on various soil factors, including texture, pH, and organic matter content.[25] Unbound particles that are not retained at the surface have the potential to migrate to deeper soil layers.[26]

It is important to note that most research is focused on the behavior of ZnO NPs in aqueous media or the solid phase of soil. To our knowledge, the effect of soil solutions on these materials is still poorly understood. However, the soil solution is the matrix in which reactions occur, making its investigation important. Soil solutions transport chemical species to and from soil particles and provide contact between solutes and soil particles.[27]

We chose three distinct soil types based on the World Reference Base for Soil Resources (WRB): Chernozem,

Regosol, and Solonetz. Chernozem, covering 1.8% of the Earth's land, is prized for its crumbly structure and fertile humus layer, prevalent in Asian and Eastern European steppes.[28] Regosol, constituting approximately 2% of land, is found on hill slopes in the Middle East and Eastern Europe, characterized by high organic matter, sandy texture, and a reddish-brown hue.[29] Solonetz, making up about 1% of land, thrives in arid climates of North America and Eastern Europe, known for its alkaline nature and salt accumulation.[30]

This work aims to examine the behavior of commercially available ZnO NPs in artificially prepared soil solutions derived from Chernozem, Regosol, and Solonetz soils. The investigation centers on the interaction between these soil solutions and ZnO NPs, specifically focusing on the changes in the structural and textural characteristics of NPs. Their stability, including their morphology, crystalline composition, surface features, and optical propertiesis also investigated. Given the widespread application of ZnO NPs as photocatalysts, their photocatalytic activity is also scrutinized following their interaction with soil solutions.

2. Materials and methods

2.1. Materials

ZnO powders were acquired from Sigma Aldrich with 99% purity. Ultrapure Millipore Milli-Q (MQ) water was used to prepare the soil solutions (18.2 MΩ cm^{-1}). The model pollutant used for determining photocatalytic activities was phenol (>99%) obtained from VWR.

2.2. Soil solution preparation and analysis

Soil sampling and analysis is detail in the ESI.†

Soil solutions were prepared using MQ water with a solid-to-solution ratio of 1 : 2.5. The mixtures were shaken with a tube rotator for 18 hours, centrifuged at 3400 rpm, and then filtered through a 0.45 µm cellulose nitrate membrane. The pH of the soil solution was measured using a digital pH meter (Inolab pH 720), and the E_c was determined using a conductivity meter (Orion 3-Star, Thermo Electron Corporation). The chemical oxygen demand (COD) values were determined following the Hungarian standards (MSZ) as provided in the ESI.† Ionic strengths (IS) were calculated using eqn (1) based on the electrical conductivity (E_c) results:

$$IS = E_c \cdot 0.0127 \qquad (1)$$

where IS is the ionic strength (mol L^{-1}) and E_c is the electrical conductivity (mS cm^{-1}).[31]

The major element content (Na, K, Ca, Mg, Zn) of the soil solutions was analyzed by inductively coupled plasma optical emission spectroscopy (ICP-OES) (Perkin Elmer Optima 7000DV), with Ar serving as the carrier gas, and with inductively coupled plasma mass spectroscopy (ICP-MS) (Agilent 7900) with He as a collision gas and Ar as the carrier gas. To determine the

This journal is © The Royal Society of Chemistry 2025

Environ. Sci.: Nano, 2025, **12**, 1328–1339 | 1329

concentration of NO_3^-, flow injection analysis (FIA) measurements were conducted using a Foss FIA Star 5000 spectrometer with an NH_4Cl buffer at pH 8.5 as the reagent. For PO_4^{3-} determination, $SnCl_2$ and $(NH_4)_6Mo_7O_{24}$ were used as reagents. Additionally, a Dionex ICS-1600 ion chromatograph (IC) was employed to measure the concentrations of F^-, Cl^-, NH_4^+, and SO_4^{2-}. The eluent composition used for the IC was 0.5 M Na_2CO_3 and 0.5 M $NaHCO_3$.

2.3. Characterization of ZnO NPs

The nanomaterials were characterized using various techniques. X-ray diffraction (XRD) patterns were recorded using a Rigaku Miniflex II diffractometer with a Cu-Kα radiation (λ = 1.5406 Å). Data points were taken in the 2θ = 20–80° range at a scan speed of 1 min^{-1}. Primary crystallite sizes were calculated using the Scherrer equation.[32]

The morphology was examined using a Hitachi S-4700 type II scanning electron microscope (SEM) after coating the samples with gold NPs (<10 nm).

Surface changes were investigated using an infrared spectrometer (IR; Bruker Equinox 55). The samples, along with KBr powder, were pressed into pellets, and the IR spectra were recorded with a resolution of 2 cm^{-1}.

Diffuse reflectance spectra (DRS) were recorded with a JASCO-V650 spectrophotometer using $BaSO_4$ as a reference, and the bandgap energy was calculated based on the Kubelka–Munk method.[33]

Data for the X-ray photoelectron spectroscopy (XPS) was collected using a Specs XPS equipment, which was outfitted with an Phoibos 150 hemispherical electron analyzer and an XR50 dual anode X-ray source. 150 W of power was used to run the Al Kα source. To eliminate sample charging during X-ray irradiation, an electron flood gun was employed. A pass energy of 100 eV was used to acquire the survey spectra, while a pass energy of 20 eV was used to collect the high resolution spectra. Version 2.3.25PR1.0.45 of the CasaXPS software was used for the evaluation. At a binding energy of 284.8 eV, the aliphatic component of the C1s spectrum served as an inner reference.

The ζ potential of the NPs was assessed using a Horiba SZ-100 nanoparticle analyzer (Retsch Technology GmbH, Germany), within a carbon electrode cell. The ζ potential values were obtained employing the Smoluchowski model, with a measured dispersion concentration of 0.001 w/v%. The hydrodynamic diameter (HD) of ZnO NPs was determined *via* dynamic light scattering (DLS) using the same analyzer and concentration.

A solution of ZnO NPs at a concentration of 1 g L^{-1} was combined with a phenol solution with an initial concentration (c_0) of 0.1 mM. The mixture was then sonicated for 10 minutes. Subsequently, the suspension was transferred into a double-walled glass vessel with a volume of 100 mL, which was surrounded by six fluorescent UV tubes (λ_{max} = 365 nm; Vilber-Lourmat T-6 L UV-A, 6 W). To achieve

adsorption–desorption equilibrium, the suspension was stirred in the dark for 10 minutes before switching on the lamps. The concentration of phenol was monitored using a high-performance liquid chromatograph (HPLC), (Merck Hitachi L-4250) The flow rate was set to 0.7 cm^3 min^{-1}, and the detection wavelength was 210 nm. The eluent used was a 70 : 30 (v/v) mixture of methanol and water.

2.4. Soil solution experiments

Each soil solution was prepared by combining the 10 samples we took from their (Chernozem, Regosol, or Solonetz) corresponding sites. As a result, we obtained a single homogeneous representative sample for each soil solution type. Stock suspensions containing 5 g L^{-1} ZnO NPs were prepared using MQ water. The ZnO-containing soil solutions were then subjected to ultrasonic treatment for 10 minutes. Subsequently, the ZnO NP concentration in the soil solutions was adjusted to 1 g L^{-1}. The suspension concentrations were chosen to be comparable with ones frequently applied in the literature.[34,35] Following the addition of the ZnO-containing stock suspension to the soil solution, the resulting mixture was stirred using a magnetic stirrer, which was protected from light. After 4 hours of interaction between the ZnO NPs and the soil solutions, the suspensions were centrifuged at 3700 rpm for 10 minutes. The properties of ZnO NPs in the soil solutions were examined using the techniques detailed in section 2.3.

3. Results and discussion

3.1. Properties of soil solutions and their possible effects on ZnO NPs

The Regosol soil solution (REG) was found to be acidic, possibly because the Regosol soil samples (which form the basis of REG) were collected from forested areas with high biomass turnover and soil acidification caused by microbial decomposition products.[36] Following chemical reactions with the environment, Zn^{2+} ions are formed which are soluble in aqueous media. There are several ZnO species, including Zn^{2+}, $ZnOH^+$, $Zn(OH)_2$, and $Zn(OH)_3^-$, whose concentrations depend on the pH levels.[37]

In acidic conditions, Zn^{2+} is the dominant species. The solubility of ZnO is determined by the degree of ZnO hydrolysis to form Zn^{2+}:

$$ZnO + 2H^+ \rightarrow Zn^{2+} + H_2O$$

The pH of the Chernozem soil solution (CH) is slightly alkaline. In near-neutral pH conditions, ZnO is considerably less soluble compared to its solubility in acidic conditions. However, even at a pH of 7.75, there may still be a small amount of dissolution, leading to the release of Zn^{2+}.[38] This is because natural water contains trace amounts of H^+ ions, which can slightly increase the acidity of the solution.[39]

The pH of Solonetz soil solution (SOL) is strongly alkaline. This high pH value is mostly due to the high cation

1330 | *Environ. Sci.: Nano*, 2025, **12**, 1328–1339

This journal is © The Royal Society of Chemistry 2025

concentration of the soil, from which the solution was prepared. At this pH, the OH^- ions are more likely to interact with Zn^{2+} ions, forming $Zn(OH)_2$ precipitates rather than soluble complexes:[40]

$$Zn^{2+} + 2OH^- \rightarrow Zn(OH)_2$$

ZnO NPs can dissolve to form zinc hydroxide complexes.[38]

The IS of the soil solutions also varies significantly. The ISs of REG and CH are considered low (Table 1). At low IS, the dominant factor is the electrostatic repulsion between charged NPs. This repulsion helps prevent aggregation and stabilizes the colloidal suspension. The lower concentration of ions in the solution under low ionic IS conditions may facilitate faster dissolution, particularly if the pH is acidic.[25] Conversely, the high IS in the solution of SOL can reduce the electrostatic repulsion between the NPs, thereby making them more prone to aggregation.[41] Additionally, the relatively high concentration of ions in high IS conditions may suppress dissolution, resulting in a slower dissolution rate.[41]

The COD concentrations in soil solutions reflect their organic matter content. High values in REG are attributed to substantial biomass turnover.[42] Similarly, elevated COD in SOL is linked to Na^+ ions mobilizing organic matter, forming soluble sodium humate complexes.[43] Humic acid enhances ZnO stability in liquid phases by increasing repulsive energy and creating an energy barrier NPs.[44,45] Organic matter also affects ZnO photocatalytic activity by adsorbing onto nanoparticles, hindering access to active sites.[46]

Inorganic ion concentrations varied: Na^+ in REG and CH is moderate but high in SOL due to specific soil characteristics.[47] Elevated Na^+ can passivate ZnO surfaces, reducing reactivity.[48] High-valent cations (Ca^{2+}, Mg^{2+}) compete with H^+ ions for ZnO surface adsorption, stabilizing suspensions at high IS values.[49]

Anion concentrations also varied: NO_3^- in CH indicates intensive nitrate fertilization, while low NO_3^- in SOL may stem from hindered nitrifying bacteria activity due to elevated Na^+.[50] PO_4^{3-} in REG is high due to increased mobility in acidic conditions.[51] Elevated Cl^- and SO_4^{2-} in

SOL result from salt accumulation, affecting ZnO behavior by adsorption and contributing to aggregation and formation of less soluble complexes.[52–54]

3.2. Crystal structure, morphology and optical properties of ZnO NPs

In the following sections, we will discuss the interaction of ZnO NPs with soil solutions and their photocatalytic activity. Pure ZnO NPs were used as a reference.

Starting with the crystal structure, each ZnO sample displayed distinct crystallographic planes corresponding to the hexagonal wurtzite structure. Diffraction peaks were observed at 31.83° (100), 34.50° (002), 36.30° (101), 47.61° (102), 56.67° (110), 62.86° (103), 66.45° (200), 68.05°, and 69.20° (112). However, as depicted in Fig. 1, there is an alteration in the intensity of reflections after the interaction of ZnO with soil solutions. The three most prominent diffraction peaks, which influence the characteristic crystal structure of wurtzite ZnO, exhibit a broadening compared to those of ZnO_REF. It does not induce crystallization in the material but signifies a change in surface quality.[55] No significant changes were observed in any of the samples after interaction with the soil solutions: reflections do not disappear and new ones do not emerge (i.e., no new material is formed, nor does the structure collapse).

After immersion in the soil solutions, the primary crystallite sizes of ZnO NPs decreased (Table 2). As discussed in section 3.1., ZnO NPs are not stable under certain conditions. Therefore, this phenomenon could be explained by the release of Zn^{2+} under acidic conditions (ZnO_REG)[56] and the formation of $Zn(OH)_2$ under alkaline conditions (ZnO_CH and ZnO_SOL).[40]

Fig. 2 presents SEM micrographs illustrating the morphology of the samples. The original polycrystalline morphology remains unchanged after interaction with the soil solutions. However, aggregation is observed, particularly noteworthy for ZnO_REG and ZnO_SOL. The soil solutions that interacted with these NPs had a notable COD content, suggesting that the interaction between ZnO NPs and organic

Table 1 Chemical properties of soil solutions

Parameters		REGOSOL soil solution (REG)	CHERNOZEM soil solution (CH)	SOLONETZ soil solution (SOL)
pH		4.95 ± 0.1	7.74 ± 0.2	9.4 ± 0.2
IS (mmol L^{-1})		1.99 ± 0.1	3.96 ± 0.1	12.03 ± 0.3
COD	mg L^{-1}	165 ± 1.2	20.9 ± 0.4	227.2 ± 1.6
Na^+		2.61 ± 0.5	8.31 ± 0.3	73.4 ± 1.1
K^+		38.35 ± 0.8	5.59 ± 0.1	94.5 ± 1.8
Ca^{2+}		32.62 ± 0.9	57.61 ± 0.1	82.65 ± 0.4
Mg^{2+}		9.84 ± 0.2	6.61 ± 0.1	26.37 ± 0.3
NO_3^-		21.55 ± 0.1	74.61 ± 0.7	24.6 ± 0.2
PO_4^{3-}		1.33 ± 0.2	0.98 ± 0.2	0.65 ± 0.1
F^-		0.13 ± 0.02	0.62 ± 0.04	0.54 ± 0.1
Cl^-		3.45 ± 0.05	9.61 ± 0.2	15.51 ± 0.4
SO_4^{2-}		1.73 ± 0.3	3.2 ± 0.15	4.56 ± 0.1
Zn^{2+}	µg L^{-1}	n.d.[a]	4.46	n.d.[a]

[a] n.d. – not detected.

This journal is © The Royal Society of Chemistry 2025

Environ. Sci.: Nano, 2025, 12, 1328–1339 | 1331

Fig. 1 XRD patterns of ZnO NPs a) before and after interaction with soil solutions, b) changes in the intensity of reflections.

compounds could lead to surface modification and aggregation.[57] The nature of the organic matter plays a crucial role, acting either as a stabilizing or destabilizing agent and potentially accelerating sedimentation.[58]

The optical characteristics of the materials were investigated to gather information on their light absorption and bandgap. The relationship between bandgap energy and light absorption is based on the absorption of photons with energies corresponding to the bandgap.[59] This phenomenon was analyzed using DRS; however, the most straightforward optical observation is through visual inspection. The color alteration of the samples after interaction with soil solutions is depicted in Fig. 3. While pure ZnO_REF is white, ZnO_REG and ZnO_CH exhibit a brownish hue, and ZnO_SOL is almost black. Interestingly, after undergoing phenol degradation (denoted as ZnO_SOL_AP, ZnO_REG_AP, and ZnO_CH_AP), they became lighter, indicating spectral changes (as shown in the spectra in Fig. 3, between 380 and 450 nm). Despite the color changes, which might influence light absorption, the bandgap of the samples did not undergo substantial alterations after interacting with the soil solutions: the bandgap is 3.1 eV for ZnO_REF and between 3.04 and 3.17 eV for the other samples (the exact values are given in Table S3†). This is attributed to the fact that not all additives and chemical entities attached to the surface can modify the structure of the materials.[60] Presumably, based on XRD and

SEM results, organics are adsorbed onto the surface. The presence of organic matter is also indicated by the color changes after phenol degradation, as they became lighter; this suggests that during photocatalytic degradation, the ZnO NPs started to degrade various organic compounds on their surface. Consequently, to gain deeper insights into surface chemistry alterations, aggregation, and the potential impacts of ZnO NPs, further investigations were carried out, which will be discussed in the next chapters.

3.3. Surface properties of ZnO NPs

Examining the surface chemistry of NPs after interaction in different soil solutions through IR spectroscopy offers valuable perspectives on their molecular interactions and surface functional groups.

The vibrational peaks associated with metal–oxide bonds generally appear in the 400–1000 cm^{-1} range. In our case, the bands observed at 454, 682, and 773 cm^{-1} were attributed to Zn–O bonds.[61] As there were no significant changes in this range for any sample in comparison to the reference ZnO, the spectra were normalized to this region.

As depicted in Fig. 4, samples that interacted with the soil solutions (ZnO_CH, ZnO_CH_AP, ZnO_REG, ZnO_REG_AP, ZnO_SOL, ZnO_SOL_AP) exhibited strong vibrational bonds in the 975–1200 cm^{-1} region. For instance, C=C bonds (alkenes) between 960–995 cm^{-1} may have been formed as a result of microbial activity in the soil.[62] Intense peaks were observed in the 1000–1100 cm^{-1} range, which are primarily associated with Si–O bonds. These correspond to the presence of silicon oxides in the soil. Additionally, vibrations related to C–O bonds were detected between 1080 and 1100 cm^{-1},[63] and these can be linked to long carbon-chain molecules in soil solutions, such as substances derived from plant decomposition (*e.g.*, lignin-based compounds).[64]

The bands at 1650 cm^{-1} were associated with O–H bonds. This band appeared not only in samples exposed to soil

Table 2 Primary crystallite sizes calculated based on the Scherrer-equation

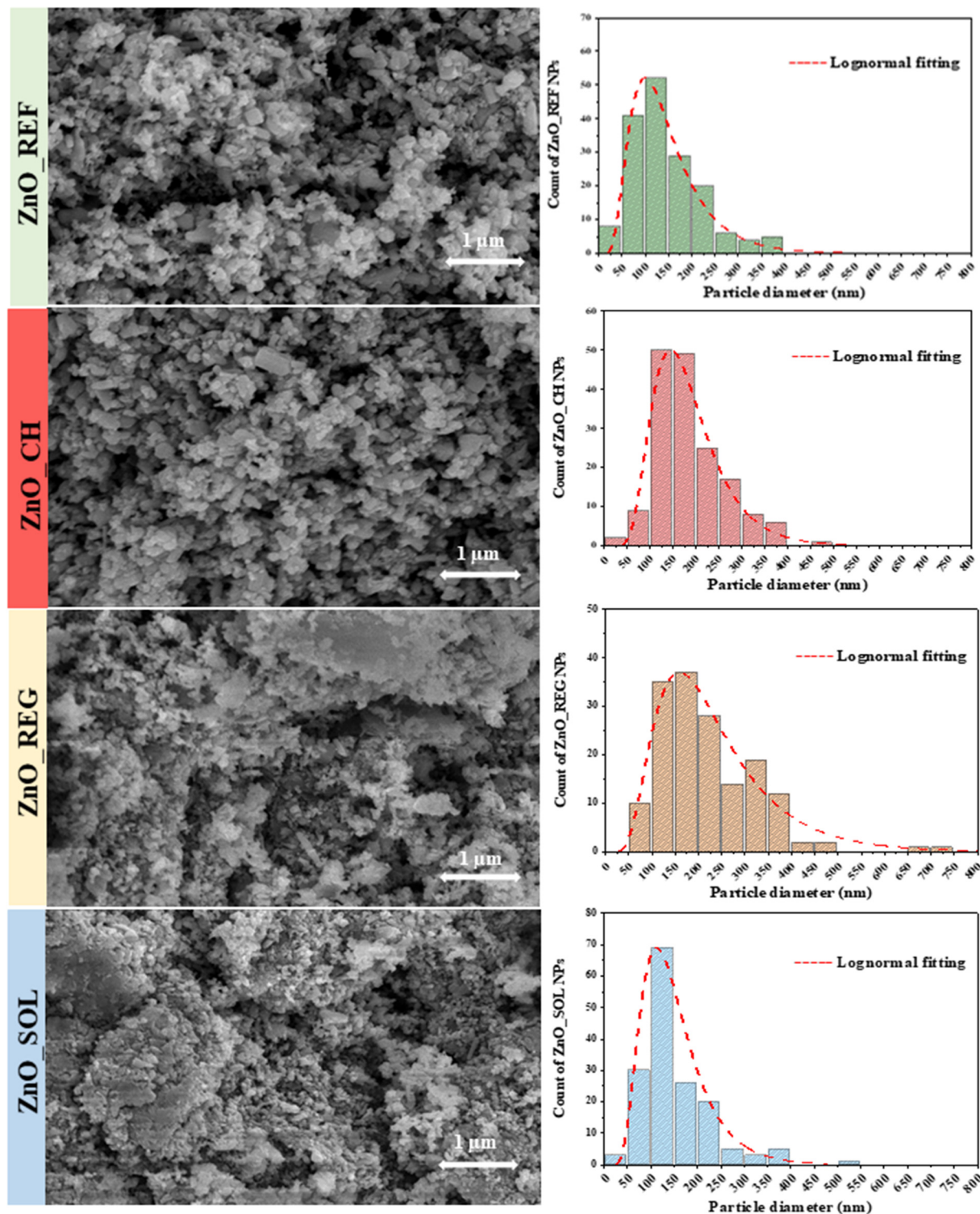| Sample name	Primary crystallite size (nm)
ZnO_REF	34.8 ± 0.7
ZnO_AP	33.5 ± 1.1
ZnO_SOL	26.3 ± 0.4
ZnO_SOL_AP	27.1 ± 0.6
ZnO_REG	28.6 ± 1.2
ZnO_REG_AP	31.5 ± 0.8
ZnO_CH	28.5 ± 0.0
ZnO_CH_AP	27.9 ± 0.4

Fig. 2 SEM micrographs of ZnO NP samples before and after immersion in soil solution, and their corresponding size distribution histograms.

solutions but also in ZnO_REF, indicating the presence of physisorbed water. The intensity of this band varied in tandem with the 3000–3500 cm^{-1} region ("water band").[45] However, the intensities of these two regions did not change simultaneously in our samples, which suggests that a compound with additional O–H groups was adsorbed on the

surface. In ZnO_AP, ZnO_REG_AP, ZnO_CH_AP, and ZnO_SOL_AP, the notable changes between these regions can be attributed to the intermediates of phenol originating from the degradation process.[65] The disappearance of the water band in ZnO_SOL might be attributed to the high ionic content of the SOL. These ions can compete with O–H groups

This journal is © The Royal Society of Chemistry 2025

Environ. Sci.: Nano, 2025, **12**, 1328–1339 | **1333**

Fig. 3 Color changes and DR spectra of ZnO NPs before and after interaction with soil solutions, and after phenol degradation: a) ZnO_SOL samples; b) ZnO_REG samples; c) ZnO_CH samples.

Fig. 4 IR spectra of ZnO NPs in the 1000–3700 cm^{-1} region.

for adsorption sites on the catalyst surface. As a result, the availability of O–H groups for hydrogen bonding with water molecules is reduced, leading to a decrease in hydrophilicity.

In all samples, vibrations indicative of CO_2 bonds at 2350 cm^{-1} were noted, stemming from the sample preparation procedure with no relevance to the analysis.[66]

Besides the IR investigations, the surface chemistry alterations were examined through ζ potential measurements too. ζ potential denotes the electric charges present on NP surfaces within a solution, impacting their stability and tendency to aggregate.[67] The ζ potential and isoelectric point (IEP) of ZnO NPs (Fig. 5) were assessed in REG, CH, SOL, and, for comparison, in distilled water (ZnO_REF).

In distilled water, the IEP of ZnO was at pH ~6.1, which is also in agreement with previous studies.[68] However, after immersion in all three soil solutions, the ζ potential was negative at pH 5. Below pH 5, we could not measure the ζ potential because in such an acidic medium the ZnO was already strongly solubilized, making the results unreliable.

Upon the immersion of ZnO NPs into soil solutions, they induced largely the same surface potential at pH 5, irrespective of the type of the soil solution. This led to the identical adsorption of species from the soil solutions onto the surfaces. Divergence in behavior becomes apparent as the
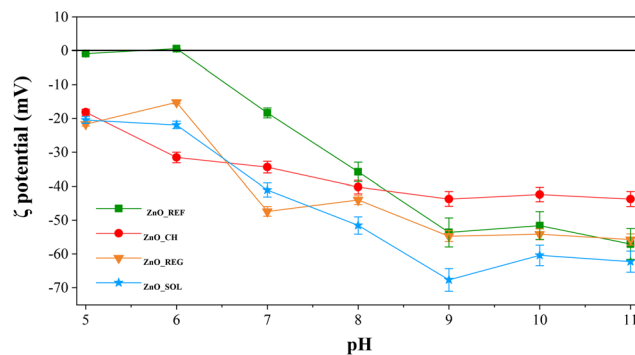

Fig. 5 ζ potential of ZnO NPs in CH, REG, and SOL soil solutions, and in distilled water.

1334 | *Environ. Sci.: Nano*, 2025, **12**, 1328–1339

This journal is © The Royal Society of Chemistry 2025

pH increases. Notably, ZnO_SOL exhibits the most negative trend, attributable to the prevalence of surface hydroxyl groups resulting from surface complexation. Despite the elevated organic content, corroborated by IR measurements revealing the presence of several OH functional groups on the surface, a similar negative trend is discernible following the interaction with REG. Although the anion content in REG does not significantly differ from the other soil solutions, its high organic matter content contributes to the observed negative potential trend, primarily attributed to surface OH groups.

However, the trend diverges when ZnO interacts with CH: above pH 7, the ζ potential is 5–10 mV higher compared to those of SOL and REG. Although CH exhibits negligible organic matter content relative to the other two, the IR results show significantly fewer adsorbed OH groups on the surface. However, the presence of anions in CH, notably, NO_3^-, F^-, and Cl^-, accounts for the sustained negative ζ potential of ZnO NPs.

After interaction with the soil solutions, the elemental composition of the surface of the ZnO NPs and what adsorbed onto the surface was investigated by XPS. The primary investigation focused on the main metal component of the oxide, *i.e.*, Zn. For Zn, there was no significant change in the 2p spectrum, so the focus was then shifted to O. The analysis of the O component shows (Fig. 6) that the amount of O–H in the post-interaction samples increased significantly, as previously shown by the IR results. This is particularly striking for the ZnO_SOL and ZnO_SOL_AP samples, confirming the hypothesis of a surface-formed amorphous hydroxyl layer.

In addition, various C-groups were also detected on the surface, mainly C–C, C–H, C–OH, C–O–C, C═O, and O–C═O functional groups (Fig. S3†), which is also confirmed by IR measurements. In the ZnO_REG sample, the intensity of the C–OH group is prominent, which was significantly contained due to the acidic nature of the REG soil solution.

The elemental composition of the surface of the samples is summarized in Table 3, where it is clearly shown that for all samples, C was the dominant element. However, an interesting trend is that after phenol degradation, the amount of C decreases for all samples, which is related to catalytic activity; the material practically cleans its own surface.

Fig. 6 O 1s XPs spectra of the ZnO samples: a) ZnO_CH, b) ZnO_CH_AP, c) ZnO_REG, d) ZnO_REG_AP, e) ZnO_SOL, f) ZnO_SOL_AP.

This journal is © The Royal Society of Chemistry 2025

Environ. Sci.: Nano, 2025, **12**, 1328–1339 | **1335**

Table 3 Element composition of ZnO NPs based on the XPS measurements

Sample name	Elemental composition[a] (a.m.%)						
	C	O	Zn	Cl	Ca	N	Na
ZnO_REF	63.17	29.85	6.98	n.d.	n.d.	n.d.	n.d.
ZnO_REF_AP	54.20	37.73	8.07	n.d.	n.d.	n.d.	n.d.
ZnO_CH	59.00	34.58	7.06	0.60	0.50	0.87	n.d.
ZnO_CH_AP	53.40	34.20	4.74	0.79	0.38	n.d.	n.d.
ZnO_REG	60.19	33.93	5.49	n.d.	n.d.	0.39	n.d.
ZnO_REG_AP	51.19	39.52	7.08	n.d.	n.d.	0.37	n.d.
ZnO_SOL	56.99	36.75	4.67	n.d.	0.70	0.56	0.32
ZnO_SOL_AP	48.37	39.74	4.46	n.d.	0.41	n.d.	0.16

[a] Percentage of atoms out of 100 for each element, n.d. = not detected.

For the CH samples, Cl was detected at the surface, which was also present in significant amounts in the CH soil solution. Ca was present in both CH and SOL samples, and its abundance was also prominent in the soil solution (this was particularly true for SOL) as well. N, which can come from both organic and inorganic forms, was either reduced or completely absent in all soil solution types after phenol degradation—a similar trend to C. In the SOL samples, we even detected Na, which was present in very high amounts in the SOL solution.

3.4. Hydrodynamic diameter of ZnO NPs

The HD of ZnO NPs interacting with soil solutions was also determined. For comparison, the ZnO NPs were also tested in distilled water (ZnO_REF). The HD value indicates the degree of surface charge compensation of the material in liquid, thereby providing insight into the material's stability. NPs with higher HD may show a higher tendency to aggregate and sediment.[69]

The HD of ZnO_REF was approximately 265 nm, slightly smaller than ZnO_SOL (273 nm) and ZnO_CH (253 nm) (all measurements had a variance of less than 7%). In contrast, the HD of ZnO_REG, with a value of 158 nm, was significantly smaller compared to that of the other samples. As already mentioned in the previous chapters, ZnO is soluble in acidic media, releasing Zn^{2+} into them. This was confirmed by our analytical results, as the Zn^{2+} content increased in REG after interaction with ZnO to 3.25 mg L^{-1}. This process is also related to the primary crystallite size, which also decreased (Table 2). However, the primary crystallite size of ZnO_SOL and ZnO_CH also decreased, while the HD did not. This may be due to the ability of ZnO to form Zn^{2+} complexes on the surface of amorphous NPs. If there is an amorphous layer on the surface of ZnO, it could not be detected by XRD, but the phenomenon is still evident from the HDs.

3.5. Photocatalytic activity of ZnO NPs

As already mentioned in the Introduction, ZnO NPs are also widely used as photocatalysts for the degradation of various organic pollutants. Therefore, we investigated the photocatalytic activity of ZnO NPs after interaction with soil solutions.

As shown in Fig. 7(a), the pure ZnO_REF sample proved to be very efficient, as it completely degraded the phenol model contaminant in about 40 minutes. The high activity of ZnO is mainly attributed to its high specific surface area, which provides more active sites for catalytic reactions, thereby enhancing the interaction between the photocatalyst and the targeted pollutants.[7]

After interaction with the CH soil solution, the photoactivity of ZnO_CH remains almost unchanged, showing a complete degradation in 40 minutes. For ZnO_REG, the activity slightly decreased, as it took about 90 minutes to degrade phenol. Only in the case of ZnO_SOL did we observe a significantly slower degradation process, as 270 minutes were required for complete degradation. The cause

Fig. 7 Phenol degradation curves of ZnO NPs: a) before and after interaction with soil solutions (CR_Phenol: phenol concentration without ZnO_NPs); b) reusability test *via* phenol degradation.

1336 | *Environ. Sci.: Nano*, 2025, **12**, 1328–1339

This journal is © The Royal Society of Chemistry 2025

for the decreasing photocatalytic activities must be related to the chemical composition of the soil solutions. As discussed in the previous sections, ZnO NPs underwent various changes after their immersion in the soil solutions.

We observed a strong relationship between the negative ζ potential, COD, and the decrease of photocatalytic activity: the higher the organic matter content of a soil solution, the more negative the ζ potential, and the lower the activity. Organic matter can negatively affect the photocatalytic activity in several ways. Firstly, organic matter can occupy active sites on the surface of ZnO NPs (this was directly observed from the IR results), resulting in a competition between the degradation of organic matter and target pollutants.[70] In addition, they can also act as electron traps for polar compounds such as hydroxyl and carboxyl groups, which tend to adsorb onto the surface of the material (also confirmed by IR measurements and indirectly by ζ potential measurements), reducing the overall efficiency of photocatalysts.[71] This effect is particularly significant in the case of hydroxyl and carboxyl groups, which tend to adsorb onto the active surface of catalysts.[72]

It is important to mention that different anions and cations also affect the photocatalytic activity of ZnO NPs. However, their exact degree of influence cannot be presented exactly, as the soil composition/thus soil solution composition may vary greatly, not mentioning the high organic matter, that also competes for the surface of the ZnO nanoparticles.[27]

After interaction with the soil solutions, a reusability test was carried out in addition to phenol degradation. This means that phenol degradation was performed again with our samples that had been previously used for degradation (Fig. 7(b)—the suffix Re for samples refers to the term reusability). The results showed that the photocatalytic activity did not decrease drastically (between ~10–25%) for the ZnO_REF_Re, ZnO_CH_Re, and ZnO_REG_Re samples compared to the first digestion (Fig. 7(a)). However, the activity efficiency of ZnO_SOL_Re samples decreased significantly by 60% compared to ZnO_SOL. The initial activity of the ZnO_SOL sample was also weaker compared to the other samples, which is due to the complex structure of OH groups and ions on the surface.

4. Conclusion

This study aimed to investigate the effects of three different types of soil solutions on commercially available ZnO NPs. Our findings revealed a decrease in the primary crystallite size of ZnO NPs after interaction with all three types of soil solutions. In the case of the acidic solution (Regosol), the HD of the NPs also decreased, accompanied by an increase in the Zn^{2+} concentration of the solution, posing potential environmental risks.[73] Conversely, HD did not undergo significant changes during immersion in alkaline soil solutions (Chernozem and Solonetz), possibly due to surface complexation. With a higher HD, these substances tend to

sediment more rapidly, potentially depositing in deeper soil layers and groundwater. Despite structural changes in the NPs and the adsorption of various organic compounds onto their surface, they retained their photocatalytic activity. However, this raises environmental concerns, as ZnO NPs near sunlight on the soil surface can degrade surrounding organic matter, altering its chemical composition. The study contributes to a better understanding of the potential risks associated with ZnO NP exposure in soil environments, guiding efforts to mitigate their adverse effects and ensure environmental sustainability. Our results indicate that the stability of NPs changes after only a few hours of interaction, prompting the need for further investigation into their longer-term effects and changes in the environment. While this study primarily focused on the effect of soil solution chemical composition on the material, future research aims to explore the behavior of ZnO NPs from the perspective of soil physical properties, aiming for a more comprehensive understanding. This study contributes to a better understanding of the potential risks associated with ZnO NP exposure in soil environments, guiding efforts to mitigate their adverse effects and ensure environmental sustainability.

Abbreviations

ZnO_REF	Pure/reference ZnO NPs
ZnO_AP	ZnO NPs after phenol degradation
ZnO_CH	ZnO NPs after interaction with Chernozem soil solution
ZnO_CH_AP	ZnO NPs after interaction with Chernozem soil solution and phenol degradation
ZnO_REG	ZnO NPs after interaction with Regosol soil solution
ZnO_REG_AP	ZnO NPs after interaction with Regosol soil solution and phenol degradation
ZnO_SOL	ZnO NPs after interaction with Solonetz soil solution
ZnO_SOL_AP	ZnO NPs after interaction with Solonetz soil solution and phenol degradation

Data availability

The data supporting this article have been included as part of the ESI† and of the submitted manuscript. The authors declare that no other data is associated with the present manuscript.

Author contributions

Karolina Solymos: conceptualization, investigation, writing – original draft, formal analysis. Eszter Kanász: investigation. Tamás Gyulavári: investigation, writing – review & editing. Áron Ágoston: investigation. Benjámin Pálffy: investigation. Ákos Szamosvölgyi: investigation. Ákos Kukovecz: resources, funding acquisition. Zoltán Kónya: resources, funding acquisition. Zsolt Pap: conceptualization, writing – review & editing, supervision, funding acquisition.

This journal is © The Royal Society of Chemistry 2025

Environ. Sci.: Nano, 2025, 12, 1328–1339 | 1337

Conflicts of interest

There are no conflicts to declare.

Acknowledgements

References

1 J. Supramaniam, D. Y. S. Low, S. K. Wong, B. F. Leo, B. H. Goh and S. Y. Tang, *Chem. Eng. J.*, 2022, **437**, 135440.

2 D. Ghosh, M. Debbarma and S. Chattopadhyaya, *Phys. B*, 2023, **665**, 415032.

3 V. Sogne, F. Meier, T. Klein and C. Contado, *J. Chromatogr. A*, 2017, **1515**, 196–208.

4 R. Huang, S. Zhang, W. Zhang and X. Yang, *IET Collab. Intell. Manuf.*, 2021, **3**, 281–289.

5 S. Raha and M. Ahmaruzzaman, *Nanoscale Adv.*, 2022, **4**, 1868–1925.

6 N. C. T. Martins, A. Avellan, S. Rodrigues, D. Salvador, S. M. Rodrigues and T. Trindade, *ACS Appl. Nano Mater.*, 2020, **3**, 2134–2148.

7 Z. Kovács, V. Márta, T. Gyulavári, Á. Ágoston, L. Baia, Z. Pap and K. Hernadi, *J. Environ. Chem. Eng.*, 2022, **10**, 107655.

8 A. Augustyniak, J. Jablonska, K. Cendrowski, A. Głowacka, D. Stephan, E. Mijowska and P. Sikora, *Appl. Nanosci.*, 2022, **12**, 489–502.

9 H. Chittella, L. W. Yoon, S. Ramarad and Z.-W. Lai, *Polym. Degrad. Stab.*, 2021, **194**, 109761.

10 F. Gottschalk, T. Sonderer, R. W. Scholz and B. Nowack, *Environ. Sci. Technol.*, 2009, **43**, 9216–9222.

11 S. Tang, J. Wang, X. Zhu and D. Shen, *Toxics*, 2024, **12**, 48.

12 X. Wang, X. Yang, S. Chen, Q. Li, W. Wang, C. Hou, X. Gao, L. Wang and S. Wang, *Front. Plant Sci.*, 2016, **6**, 1243.

13 S. A. Al-Zahaby, M. R. Farag, M. Alagawany, H. S. A. Taha, M. V. Varoni, G. Crescenzo and S. A. Mawed, *Animals*, 2023, **13**, 2867.

14 J. Fang, X.-q. Shan, B. Wen, J.-m. Lin and G. Owens, *Environ. Pollut.*, 2009, **157**, 1101–1109.

15 K. Solymos, I. Babcsányi, B. Ariya, T. Gyulavári, Á. Ágoston, Á. Szamosvölgyi, Á. Kukovecz, Z. Kónya, A. Farsang and Z. Pap, *Environ. Sci.: Nano*, 2024, **11**, 1204–1216.

16 K. Solymos, I. Babcsányi, B. Ariya, T. Gyulavári, Á. Ágoston, Á. Kukovecz, Z. Kónya and Z. Pap, *Environ. Sci. Eur.*, 2024, **36**, 85.

17 Z. Elhaj Baddar, C. J. Matocha and J. M. Unrine, *Environ. Sci.: Nano*, 2019, **6**, 2495–2507.

18 E. Tiwari, N. Singh, N. Khandelwal, Z. A. Ganie, A. Choudhary, F. A. Monikh and G. K. Darbha, *Chemosphere*, 2022, **308**, 136091.

19 E. Lahive, M. Matzke, C. Svendsen, D. J. Spurgeon, H. Pouran, H. Zhang, A. Lawlor, M. Glória Pereira and S. Lofts, *Environ. Pollut.*, 2023, **319**, 120907.

20 Y. H. Shih, W. S. Liu and Y. F. Su, *Environ. Toxicol. Chem.*, 2012, **31**, 1693–1698.

21 M. Di Addario, I. Temizel, N. Edes, T. T. Onay, B. Demirel, N. K. Copty and B. Ruggeri, *J. Environ. Chem. Eng.*, 2017, **5**, 5944–5953.

22 F. Wu, B. J. Harper and S. L. Harper, *Environ. Toxicol. Chem.*, 2019, **38**, 591–602.

23 P. Wang, N. W. Menzies, P. G. Dennis, J. Guo, C. Forstner, R. Sekine, E. Lombi, P. Kappen, P. M. Bertsch and P. M. Kopittke, *Environ. Sci. Technol.*, 2016, **50**, 8274–8281.

24 M. F. Seleiman, A. Santanen and P. S. A. Mäkelä, *Resour., Conserv. Recycl.*, 2020, **155**, 104647.

25 M. Ermolin, N. Fedyunina and O. Katasonova, *Materials*, 2019, **12**, 1270.

26 M. Simonin, J. M. F. Martins, G. Uzu, L. Spadini, A. Navel and A. Richaume, *Sci. Total Environ.*, 2021, **783**, 146952.

27 C. Chen and R. J. Wagenet, *J. Hydrol.*, 1992, **130**, 105–126.

28 E. Eckmeier, R. Gerlach, E. Gehrt and M. W. I. Schmidt, *Geoderma*, 2007, **139**, 288–299.

29 R. Lucian, G. Nicolae and L. Mărăcineanu, *Annals of the University of Craiova*, 2021, **LXI**, 190–195.

30 J. W. Hopmans, A. S. Qureshi, I. Kisekka, R. Munns, S. R. Grattan, P. Rengasamy, A. Ben-Gal, S. Assouline, M. Javaux, P. S. Minhas, P. A. C. Raats, T. H. Skaggs, G. Wang, Q. De Jong van Lier, H. Jiao, R. S. Lavado, N. Lazarovitch, B. Li and E. Taleisnik, in *Advances in Agronomy*, ed. D. L. Sparks, Academic Press, 2021, vol. 169, pp. 1–191.

31 Y. Qiu, Z. Mu, N. Wang, X. Wang, M. Xu and H. Li, *Sci. Total Environ.*, 2020, **731**, 139215.

32 V. Uvarov and I. Popov, *Mater. Charact.*, 2007, **58**, 883–891.

33 R. Alcaraz de la Osa, I. Iparragirre, D. Ortiz and J. M. Saiz, *ChemTexts*, 2019, **6**, 2.

34 G. Kovács, L. Baia, A. Vulpoi, T. Radu, É. Karácsonyi, A. Dombi, K. Hernádi, V. Danciu, S. Simon and Z. Pap, *Appl. Catal., B*, 2014, **147**, 508–517.

35 T. Gyulavári, Z. Pap, G. Kovács, L. Baia, M. Todea, K. Hernádi and G. Veréb, *Catal. Today*, 2017, **284**, 129–136.

36 H. M. Meena and H. C. Prakasha, *J. Plant Nutr.*, 2022, **45**, 358–368.

37 J. Han and K. Ogle, *J. Electrochem. Soc.*, 2017, **164**, C952.

38 H. Kaya, R. B. Karabacak, Y. Çelik, J. Peake, S. Watkins, R. Sayer and E. Suvacı, *Microchem. J.*, 2023, **191**, 108772.

39 D. Cardoso, A. Narcy, S. Durosoy, C. Bordes and Y. Chevalier, *Powder Technol.*, 2021, **378**, 746–759.

40 A. W. Mossa, D. Gashu, M. R. Broadley, S. J. Dunham, S. P. McGrath, E. H. Bailey and S. D. Young, *Soil*, 2021, **7**, 255–268.

41 D. Gentili and G. Ori, *Nanoscale*, 2022, **14**, 14385–14432.

1338 | *Environ. Sci.: Nano*, 2025, **12**, 1328–1339

This journal is © The Royal Society of Chemistry 2025

42 Y. Hu, Q. Zheng, L. Noll, S. Zhang and W. Wanek, *Soil Biol. Biochem.*, 2020, **141**, 107660.

43 D. L. Sparks, in *Environmental Soil Chemistry*, ed. D. L. Sparks, Academic Press, Burlington, 2nd edn, 2003, pp. 285–300, DOI: **10.1016/B978-012656446-4/50010-4**.

44 C. S. Rahale, A. Lakshmanan, M. G. Sumithra and E. R. Kumar, *Solid State Commun.*, 2021, **333**, 114355.

45 H. Dai, T. Sun, T. Han, Z. Guo, X. Wang and Y. Chen, *Environ. Res.*, 2020, **191**, 110086.

46 Y. Sun, W. Zhang, Q. Li, H. Liu and X. Wang, *Adv. Sens. Energy Mater.*, 2023, **2**, 100069.

47 D. L. Sparks, B. Singh and M. G. Siebecker, in *Environmental Soil Chemistry*, ed. D. L. Sparks, B. Singh and M. G. Siebecker, Academic Press, Boston, 3rd edn, 2024, pp. 411–438, DOI: **10.1016/B978-0-443-14034-1.00010-1**.

48 M. Abdullah, G. K. C. Low and R. W. Matthews, *J. Phys. Chem.*, 1990, **94**, 6820–6825.

49 X. Wang, T. Sun, H. Zhu, T. Han, J. Wang and H. Dai, *J. Environ. Manage.*, 2020, **267**, 110656.

50 A. Nejidat, *FEMS Microbiol. Ecol.*, 2005, **52**, 21–29.

51 P. D. Johan, O. H. Ahmed, L. Omar and N. A. Hasbullah, *Agronomy*, 2021, **11**, 2010.

52 X. Qian, Z. Gu, Q. Tang, A. Hong, Z. Xu, Y. Dai, X. Bian, H. Lou, M. Mortimer, M. Baalousha and L. Li, *J. Hazard. Mater.*, 2021, **410**, 124568.

53 Z. Luo, S. Zhu, Z. Liu, J. Liu, M. Huo and W. Yang, *J. Water Health*, 2015, **13**, 704–713.

54 T. K. Le, T. M. T. Nguyen, H. T. P. Nguyen, T. K. L. Nguyen, T. Lund, H. K. H. Nguyen and T. K. X. Huynh, *Arabian J. Chem.*, 2020, **13**, 1032–1039.

55 T. Ungár, *Scr. Mater.*, 2004, **51**, 777–781.

56 L. Al-Farsi, T. M. Souier, M. Al-Hinai, M. T. Z. Myint, H. H. Kyaw, H. M. Widatallah and M. Al-Abri, *Nanomaterials*, 2022, **12**, 3735.

57 M. Sikder, J. Wang, B. A. Poulin, M. M. Tfaily and M. Baalousha, *Environ. Sci.: Nano*, 2020, **7**, 3318–3332.

58 Z. Xu and D. C. W. Tsang, *Eco-Environ. Health*, 2024, **3**, 59–76.

59 A. R. Zanatta, *Sci. Rep.*, 2019, **9**, 11225.

60 T. M. Magne, T. de Oliveira Vieira, L. M. R. Alencar, F. F. M. Junior, S. Gemini-Piperni, S. V. Carneiro, L. M. U. D. Fechine, R. M. Freire, K. Golokhvast, P. Metrangolo, P. B. A. Fechine and R. Santos-Oliveira, *J. Nanostruct. Chem.*, 2022, **12**, 693–727.

61 K. Sowri Babu, A. Ramachandra Reddy, C. Sujatha, K. Venugopal Reddy and A. N. Mallika, *J. Adv. Ceram.*, 2013, **2**, 260–265.

62 Y. Yang, J. Geng, S. Cheng, H. Fang, Y. Guo, Y. Li, Y. Zhou, F. Shi and K. Vancampenhout, *Geoderma*, 2023, **431**, 116359.

63 Z. Zhu, B. Minasny, D. J. Field and S. An, *Catena*, 2023, **231**, 107366.

64 W. Machado, J. C. Franchini, M. de Fátima Guimarães and J. T. Filho, *Heliyon*, 2020, **6**, e04078.

65 O. Abbas, G. Compère, Y. Larondelle, D. Pompeu, H. Rogez and V. Baeten, *Vib. Spectrosc.*, 2017, **92**, 111–118.

66 A. Iskra, A. S. Gentleman, A. Kartouzian, M. J. Kent, A. P. Sharp and S. R. Mackenzie, *J. Phys. Chem. A*, 2017, **121**, 133–140.

67 M. Samari-Kermani, S. Jafari, M. Rahnama and A. Raoof, *Colloid Interface Sci. Commun.*, 2021, **42**, 100389.

68 R. Marsalek, *APCBEE Proc.*, 2014, **9**, 13–17.

69 N. Izadi, M. M. M. Sangani, M. A. Yavari and M. Baghdadi, *Environ. Technol. Innovation*, 2023, **30**, 103119.

70 D. Rajamanickam and M. Shanthi, *Arabian J. Chem.*, 2016, **9**, S1858–S1868.

71 U. K. H. M. Nadzim, N. H. H. Hairom, M. A. H. Hamdan, M. K. Ahmad, A. A. Jalil, N. W. C. Jusoh and S. Hamzah, *J. Alloys Compd.*, 2022, **913**, 165145.

72 D. S. Bohle and C. J. Spina, *J. Am. Chem. Soc.*, 2009, **131**, 4397–4404.

73 R. Belal and A. Gad, *Sci. Rep.*, 2023, **13**, 3520.

This journal is © The Royal Society of Chemistry 2025

Environ. Sci.: Nano, 2025, **12**, 1328–1339 | **1339**